SHEAR COATING TECHNOLOGY FOR PRODUCING HIGHLY ORDERED COLLOIDAL NANOCOMPOSITE USING ETPTA MONOMER

By

ZHEN LIU

A THESIS PRESENTED TO THE GRADUATE SCHOOL OF THE UNIVERSITY OF FLORIDA IN PARTIAL FUIFULLMENT OF THE REQUIREMENT FOR THE DEGREE OF MASTER OF SCIENCE

UNIVERSITY OF FLORIDA

2017

To my parents
Xu Liu and Xiaoyan Li

ACKNOWLEDGEMENTS

On the outset, I would like to thank my professor Dr. Peng Jiang. Thank you for giving me an opportunity to be your student and presenting me a great subject which I am really interested in. Thank you for guiding me and teaching me. Thank you for trusting me in exploring the subject which I am new to.

I would like to appreciate great support by Sin-yen Leo and Zhuxiao Gu. The great assistance they provided promotes the accomplishment of my subject. I am thankful to Dr. Yiider Tseng, Tian Lan for providing me with the access to AI Rheometer, which is also significant for my research. Besides, I would like to thank my group members for helping me whenever difficulties encountered.

I would like to thank my parent, Xu Liu and Xiaoyan Li, sincerely. Thank you for offering me an opportunity to study aboard in the US. I will greatly cherish it and take it as treasure in my life. I would also appreciate my girlfriend Sitong Liu for keeping me accompany and providing me with constant support and understanding.

Last but not least, I would appreciate Department of Chemical Engineering and University of Florida. I will stay strong in the future under the great care you presented.

TABLE OF CONTENTS

LIST OF FIGURES

Abstract of Dissertation Presented to the Graduate School
of the University of Florida in Partial Fulfillment of the
Requirements for the Degree of Master of Science

SHEAR COATING TECHNOLOGY FOR PRODUCING HIGHLY ORDERED COLLOIDAL NANOCOMPOSITE USING ETPTA MONOMER

By

Zhen Liu

Chair: Peng Jiang
Major: Chemical Engineering

A novel method of coating will be introduced, which is called Shear Coating. Shear Coating represents an efficient technology, which leads to 3D highly ordered crystal-monomer nanocomposites, or macroporous polymer membranes. With the comparison with the other coating method, Shear Coating has its great advantages for its efficiency, simplicity, and saving time. Two glass substrates are needed during the coating process, which includes with Squeeze procedure and shear procedure. Dynamic transport analysis will further be demonstrated to make the procedures clear and understandable. The thickness of the sample can be controlled by placing defined spacer between two glass substrates and the other variables will also be discussed further, such as shear rate, number of shearing cycle, volume fraction of nanoparticle, etc. The optical properties can be tested by Spectrometer, and the spectrum result can be well explained by theoretical prediction, which is Bragg's Law. SEM characterization and Bonding order parameter are also involved to test the nanostructure of nanocomposite.

CHAPTER 1
INTRODUCTION

1.1 Background Information

In nano-scaled area, it cannot deny the fact the properties vary with changing the size of particles, such as surface properties, optical properties, etc. This can be explained by the surface to volume ratio. According to Figure 1-1, which is shown above, it can be seen that all of the three cubes share the same volume. However, smaller particle inside will lead to a much larger surface area, which will determine the interaction between the particle and other molecules and all kinds of different surface. These new properties are crucial for the behavior of the particles during the different stages of production, processing and final application.

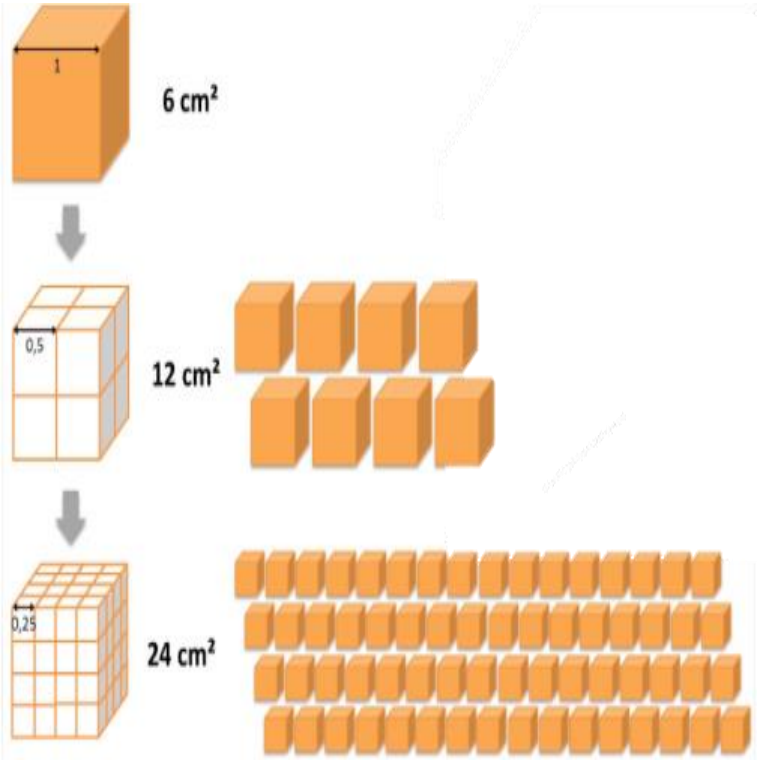

Figure 1-1. Same volume, higher surface area: several areas: several small particles have a higher surface area compared to one large particle.

The surface of a particle not only affects the physical chemical behavior of a nanomaterial, such as reactivity, solubility, and the biological properties, such as compatibility with tissues (in medical applications), but also the surface also determines the level of interactions between the particle and other molecules and all kinds of different surfaces. Due to the wide variety of surface coatings available worldwide, the nano-objects' properties can be tailored with regard to a specific application. As a consequence, coating is the main method for characterizing the optical properties. As a result, different kinds of coating play a crucial role in both experimental and industrial field.

In order to create highly quality colloidal nanocomposites, lots of coating methods are designed to achieve self-assembly property of nanoparticle, including gravitational sedimentation, [1] capillary-force-induced self-assembly, [1-5] electro- static repulsion, [6] physical confinement, [7,8] electric- and magnetic-field-assisted assembly, [9, 10] shear-force-induced ordering, etc. However, all the method above can be valid only for low-volume, laboratory-scale production, or small coating area. Besides, the methods above cannot achieve efficient goal in industrial production. Technical incompatibility with mature microfabrication is another major issue for current colloidal self-assemblies. The issues above are too serious to be negligible. Therefore, an efficient, timesaving, and high-quality method is significant for both laboratory field and industry field.

In order to solve the issues above, spin coating technology was developed. A large scale of nanocomposite can be easily fabricated rapidly with a simple spin coater (Figure 1-2). An ideal uniform film can be obtained with the centrifugal force serving as the driving force and the thickness of the film can be solved by Stokes Equation. However, [11, 12, 13] the spin coating

system is a batch reactor, which is the main drawback. A continuous and compatible process is in great needed, especially in industrial field.

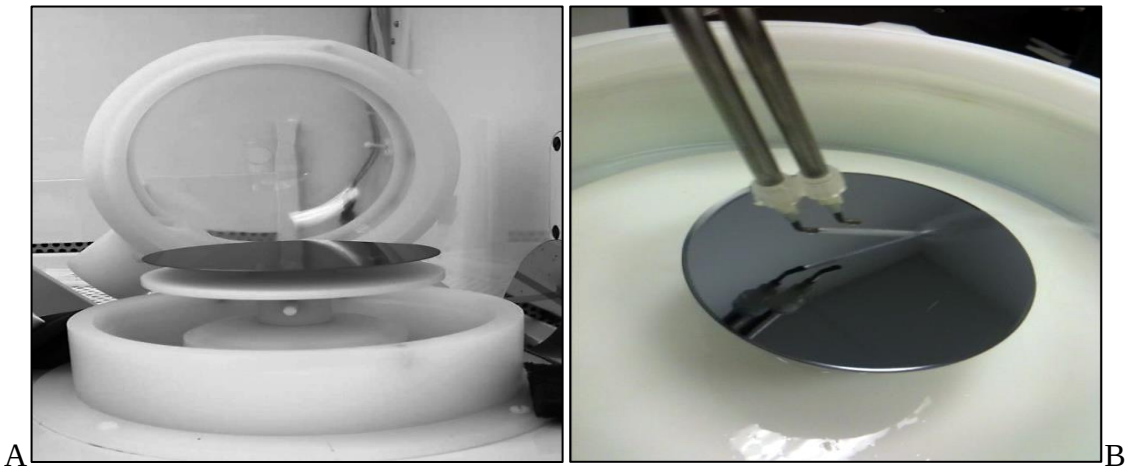

Figure 1-2. Spin coating technology. A) A standard spin coating equipment, B) A silicon wafer as a template during the spin coating process.

The other important coating method belongs to Evaporation Induced Self Assembly (EISA), [14] which can be seen from Figure 1-3. In this system, capillary force is the main driving force. Evaporation will help the silica particles to achieve self-assembly on the glass substrates with the liquid evaporating. It is a quite simple way to achieve self-assembly with the help of capillary force, but it cannot be a timesaving method unless heat or vacuum condition is applied to the system. What's more, EISA can only valid for a low volume colloidal crystal, which means that EISA can hardly be applied to the industry.

Doctor Blade Coating seems like a prefect way. [15] It is a roll-to-roll process, which can be widely applied to the industry. It can also be used in scale-up process. The thickness of the film varies with changing the speed of the blade, the distance of the gap, etc. In this case, The Doctor Blade Coating shows a great advantage for its experimental process. It is really easy to be performed.

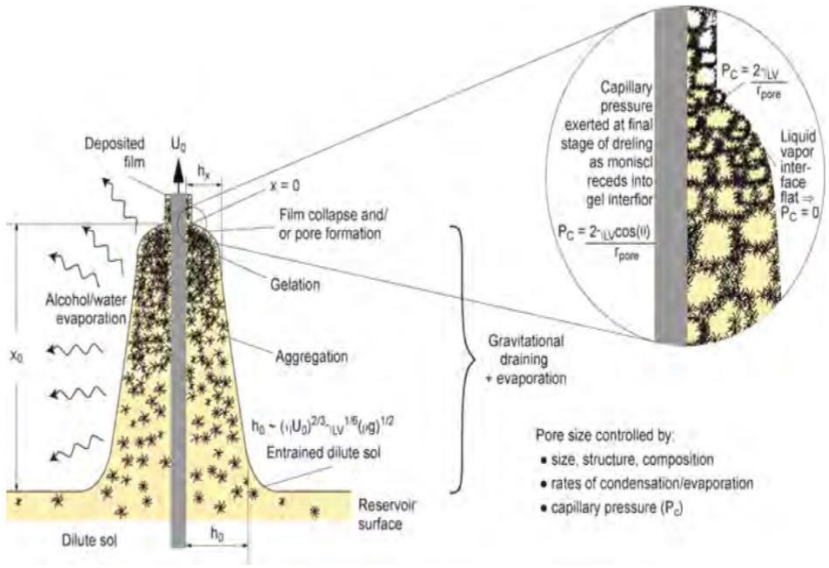

Figure 1-3. Evaporation Induced Self-Assembly

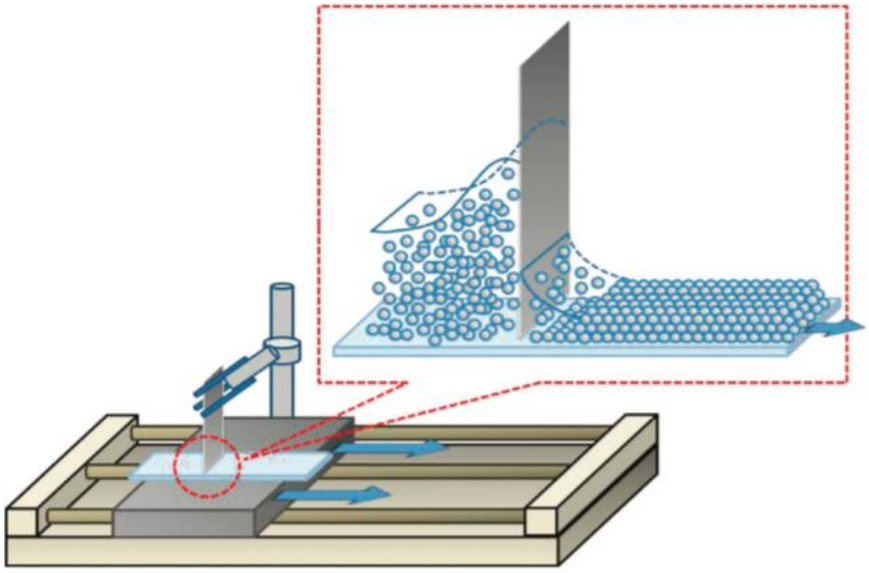

Figure 1-4. Schematic illustration of the experimental setup for assembling large-area colloidal crystal-polymer nanocomposites using a simple doctor blade coating technique.

[16-20] Inspired by the Doctor Blade Coating. Here I will introduce a novel method of coating, which is called Shear Coating. Shear Coating was used many years ago in fabrication of opals (Figure 1-5).

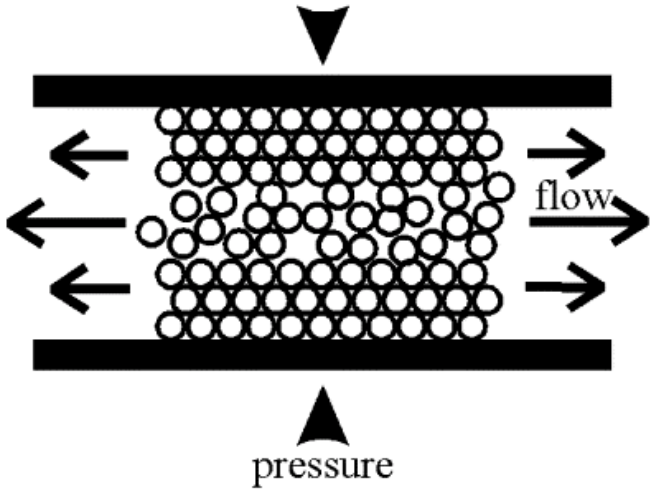

Figure 1-5. Schematic illustration of shear coating technique.

Shear coating can be applied to many areas, such as textile, paper, ceramic, etc. In shear coating, two glass substrates move relatively with colloidal suspension in between. The shear force can be unidirectional during the shear process. A spacer can be applied to the system to control the thickness of film. Inspired by this technology, a novel technology will be report in this thesis for fabricating crystal-polymer nanocomposites and macroporous polymer membrane. The resulting 3D sample shows great reflection intensity, which fits Bragg's Law well.

1.2 Objectives

The main goal of this thesis is to provide a novel coating method, which is called shear coating, which can be applied in ceramic, glass substrates, etc. With the shear force and compression acted as driving force, a sample with great quality can be easily fabricated.

1. Fabricate the ETPTA nanoporous structure by colloidal-suspension synthesis, shear coating technology and wet etching process.

2. Test the optical properties of the nanoporous polymer with spectrometer, which matches Bragg's Law.

3. Understand the complex fluid modeling during the experiment, and get the velocity expression by Navier-Stokes Equation.

4. Understand the principle of rheology measurement and get the relationship between viscosity and shear rate.

5. SEM characterization to test the nanostructure image of the ETPTA nanoporous structure.

6. Change different variables to test the changing of the optical properties.

CHAPTER 2
EXPERIMENTAL SECTION

2.1 Materials and Substrates

All experimental chemicals were of reagent quality and were used without further purification. Ethanol (200 proof) was purchased from Pharmaco Products. Ethoxylated trimethylolpropane triacrylate monomer (ETPTA, SR 454) was obtained from Sartomer. Photoinitiator Darocur 1173 (2-hydroxy-2-methyl-1-phenyl-1-propanone) was provided by Ciba-Geigy. Glass microslides (Fisher) were cleaned in piranha solution (a 3:1 mixture of concentrated sulfuric acid and 30% hydrogen peroxide) for half an hour, rinsed with Milli-Q water (18.2 MΩ cm), and dried in a stream of nitrogen.

2.2 Instrumentations

Scanning electron microscopy (SEM) was carried out on a JEOL 6335F FEG-SEM. Photopolymerization of the ETPTA monomer was carried out on a pulsed UV curing system (RC 742, Xenon). A KD Scientific 780-230 syringe pump was used to control the coating speed precisely. The viscosity of colloidal suspensions was measured using an ARESLS-1 rheometer (TA Instruments). Oxygen plasma etching was performed on a Unaxis Shuttlelock RIE/ICP reactive-ion etcher. Normal incidence optical reflection spectra were obtained using an Ocean Optics HR4000 high-resolution fiber optic vis-near-IR spectrometer with a reflection probe.

2.3 Preparation of Colloidal Suspension

The synthesis process is called Stöber method, which is one of the most well-established method. The nanospheres with a less than 5% diameter variation can be monodispersed in solvent. Washed by 200 proof ethanol multiple times, purified silica nanospheres can be fully dispersed throughout ETPTA monomer. Few drops of hotoinitiator Darocur 1173 (2 wt%) were added to the colloidal suspension. Adjust the volume fraction of silica nanosphere from 30% to

65%. 5μm syringe filter are needed to remove large aggregated particle. Transfer the fresh colloidal suspension in an open vial, and place the open vial in the dark for 12 hours to let remaining ethanol fully evaporated.

2.4 Shear Coating

Am immobile glass substrate was placed on a flat plate. Spacer was flatly stuck on the immobile glass substrate, which served to control the thickness of final film. Approximately one-milliliter silica-ETPTA colloidal suspension was dropped on the substrate and placed another glass substrate on the top. Squeezed two glass substrates to let the gap share the same thickness with spacer. The upper substrate was dragged by a syringe pump at a control speed, and then convection took place in the colloidal suspension. Moved the upper glass substrate back and forth with KD Scientific 780-230 syringe pump. After shear procedure, intense UV radiation was needed to polymerize the ETPTA monomer rapidly. The polymer matrix could be removed by using a reactive ion etcher operating at 40 mTorr oxygen pressure, a 40 sccm flow rate, and 100 W for 10 min. Submerged the raw sample in a 2 vol % hydrofluoric acid aqueous solution for 10 hours so that silica will be fully etched. Rinsed with DI water and dried in a stream of nitrogen.

2.5 Relative Viscosity Measurements:

A 54-mm-diameter cone-plate geometry system was applied during the rheology measurement. The characterization took place with shearing the colloidal suspension under the cone-plate. The gap was constant which is 520μm in all experiments. Presheared the colloidal suspension at a relatively high shear rate (approximately $100s^{-1}$ for 300s) to achieve steady state. Test the viscosity with changing the shear rate from $0s^{-1}$ to $100s^{-1}$. The temperature stayed 25℃ during the experiments with the fluctuation less than 0.05℃.

2.6 Normal Incidence Optical Reflection Measurements:

Spectrum result was tested by an Ocean Optics spectrometer, a reflection probe, and a calibrated halogen light. Calibrated halogen light was used for illuminating the sample, and a reflection probe was used to test the intensity of reflection. The area of the beam spot could be seen on the sample with a diameter of 3mm. The measured result revealed the relative intensity of reflection, which stood for a ratio of the sample spectrum intensity to the reference spectrum intensity. The reference spectrum was the absolute reflection intensity of an aluminum-sputtered silicon wafer. The final value of the relative reflectivity was the average of several measurements obtained from different spots on the sample surface.

CHAPTER 3
CHARACTERIZATION

3.1 Rheology Characterization

Rheology is the study of flow and deformation of materials. Deformation and flow are referred to as strain and strain rate, respectively, and indicate the distance over which a body moves under the influence of an external force, or stress. For this reason, rheology is also considered to be the study if stress-strain relationships in materials.

Newtonian fluid is a fluid of which the viscous stresses are in a relationship of linearly proportion with the local stain rate, which means

$$\tau = \mu \frac{du}{dy}, \tag{3-1}$$

where τ stands for the shear stress and μ is the viscosity of the fluid. In this case, it can be assumed that the viscosity μ stays the same throughout the fluid. In order to model the fluid mechanics of the experimental process, the viscosity of the colloidal suspension is necessary to be measured.

Rheology measurements took place in the geometry of 54-mm-diameter-cone plate. Shearing the colloidal suspension with changing the shear rate is needed to characterize the rheology properties. Set the gap to 52μm in all experiments, and pre-sheared the colloidal suspension at the rate of $100s^{-1}$ for one minute to control the same initial condition, which can help to get to the steady state. Set the temperature constant at 25℃ with the fluctuation, which is less than 5% during the measurement. The rheology result can be shown below (Figure 3-1).

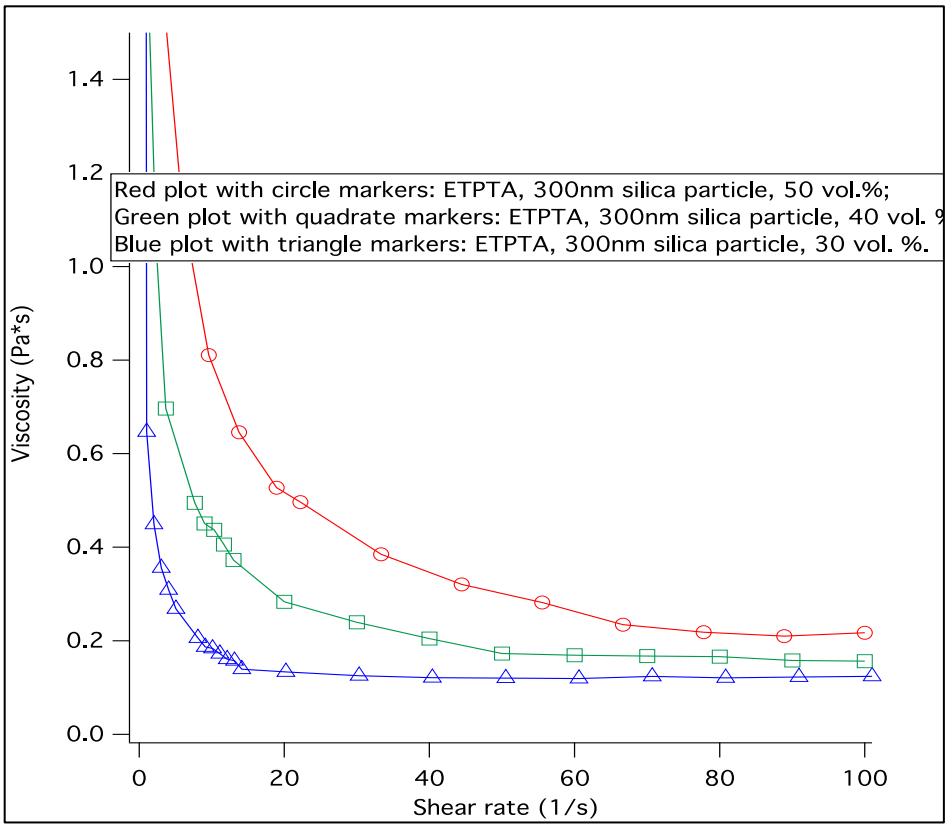

Figure 3-1. Viscosity of 300nm silica sphere/ETPTA suspensions with different particle volume fractions at various shear rates.

3.2 Spectrum Characterization

In order to testify the reflection properties of the ETPTA samples, Ocean Optics HR4000 spectrometer is necessary. Spectrometer is a scientific experimental device, which can split the light into an array of separate colors, which is called spectrum. The reflection light can be test by an optical sensor when the tested sample is illuminated. The reflection wavelength and intensity can be measured during the spectrum characterization.

An Ocean Optics spectrometer with a reflection probe was used for reflectance measurements. A calibrated halogen light source was used to illuminate the sample. The beam spot size was about 3 mm on the sample surface. Measurements were performed at normal incidence, and the cone angle of collection was less than 5 degrees. Absolute reflectivity was

obtained as a ratio of the sample spectrum to the reference spectrum. The reference spectrum was the optical density obtained from an aluminum-sputtered (1000 nm thick) silicon wafer. The final value of the absolute reflectivity was the average of several measurements obtained from different spots on the sample surface.

Lots of factors may determine the properties of the ETPTA sample, such as how many cycle of shearing, shear rate, silica sphere volume fraction, etc. The discussion about different factors will be demonstrated below.

3.2.1 Shearing Cycle

In the shear geometry, the shear force will act as the driving force, which is a kind of resultant force. The work is determined by the magnitude of shear force and the displacement that caused by the shear force, and the magnitude of displacement can be directly revealed by the number of shear cycle. Hence, it can be assumed that the number of shearing cycle may affect the reflection property. We tested that the shear cycle cannot significantly influence the reflective wavelength. The tested result is shown in Figure 3-2 and Figure 3-3..

Times of Shearing	Wavelength/nm								average peak position
5	638.4602	639.295882	620.630959	635.251184	646.692419	640.134227	644.039867	647.812041	640.6456299
10	609.79581	607.160738	611.874677	614.652969	614.79321	613.125352	620.493333	620.769531	614.1225585
15	632.878889	620.910118	621.187397	621.046591	623.832396	625.63942	619.102442	627.311059	623.3211635
20	617.432647	611.040926	618.268095	617.570909	614.374828	617.710857	620.075765	618.822813	617.3633581
30	628.56	629.54	634.415	626.89	629.4	629.68	633.44	627.03	629.6083333
40	622.16	619.52	621.19	621.75	623.83	607.72	622.02	618.96	620.9333333
50	617.155	618.13	617.154	622.16	620.22	622.02	620.07	620.91	619.7508333

Figure 3-2. Spectrum Result with changing the number of shearing cycle.

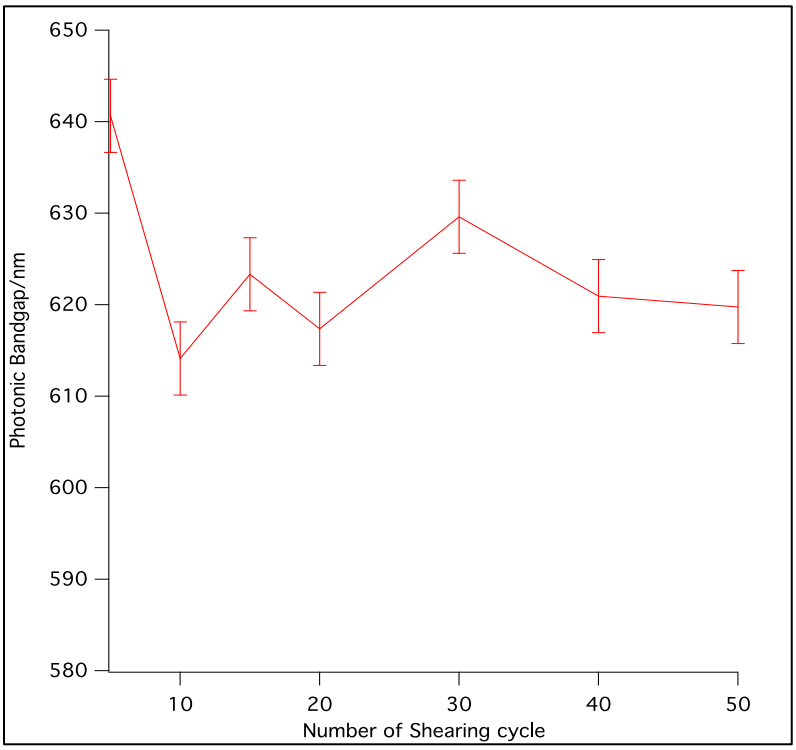

Figure 3-3. Photonic band gap (reflection wavelength) with changing the number of shearing cycle.

Testing the bandwidth is one of the major methods to measure the intensity of the reflection. The bandwidth can be measured manually on the spectrum plot. The table with values of bandwidth and the plot of the bandwidth with changing the number of shear cycles are listed below.

Times of shear	bandwith								Average	SD	
	1	2	3	4	5	6	7	8			
5	77.97	90.85	81.36	81.36	84.75	83.05	82.37	81.03	82.8425	3.52574372	3.76917858
10	77.97	77.97	78.64	75.59	79.66	78.305	80.68	82.03	78.855625	1.82464626	1.9506289
15	76.9491525	77.9661017	76.2711864	81.6949153	79.6610169	77.6271186	77.9661017	74.5762712	77.8389831	2.00500308	2.14343845
20	80.6779661	77.9661017	77.9661017	77.9661017	80.6779661	79.6610169	77.9661017	76.2711864	78.6440678	1.44813623	1.54812275
30	93.220339	84.7457627	84.7457627	92.5423729	81.3559322	85.7627119	92.8813559	86.440678	87.7118644	4.23982975	4.53256865
40	79.6610169	76.9491525	77.9661017	74.5762712	77.2881356	81.3559322	78.3050847	76.2711864	77.7966102	1.93991918	2.07386083
50	74.5762712	77.9661017	74.5762712	72.5423729	74.2372881	74.5762712	77.9661017	72.8813559	74.9152542	1.91007249	2.04195338

Figure 3-4. Bandwidth value with changing the number of shear cycles.

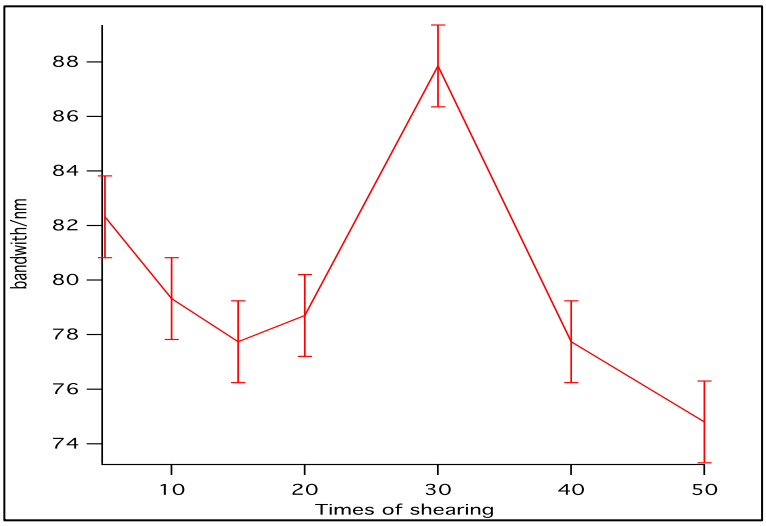

Figure 3-5. Bandwidth value of reflection with changing the number of shear cycles.

3.2.2 Shear Rate

According to the Navier-Stokes Equation, the shear rate may affect the transport result of the colloidal suspension between two substrates. The rheology data shows that the viscosity of the colloidal suspension will stay constant when shear rate reaches a certain speed, which is easy to achieve. In this case, we can assume that the colloidal suspension has the same property with the Newtonian flow. As a result, it is needed to test the result caused by shear rate.

Set an immobile glass substrate and placed few drops of colloidal suspension (about 1ml) on the glass substrate. Placed the other glass substrate on the top and squeeze the flow. Controlled the shear rate with KD Scientific Syringe Pump. The other factors are needed to stay constant in a series of experiments, such as the thickness of the sample, the pressure exerted to squeeze two glass substrates, the volume fraction of silica spheres, the diameter of the silica spheres, etc. The photonic bandgap values and the plot with changing the shear rate are listed below.

Relative Shear Rate	Photonic Bandgap/nm						Average photonic bandgap/nm
20	590.9431	591.775	589.1434	594.2682	589.418	596.344	591.98205
40	605.4947	605.495	599.808	599.8081	609.389	600.783	603.4629833
60	598.8429	597.176	598.2898	601.4799	590.117	596.347	597.0421667
80	611.1881	606.333	607.5867	605.6401	609.805	606.61	607.8604167
120	606.467	604.809	605.4989	597.3148	601.753	605.642	603.5807833

Figure 3-6. Photonic bandgap values with changing the relative shear rate.

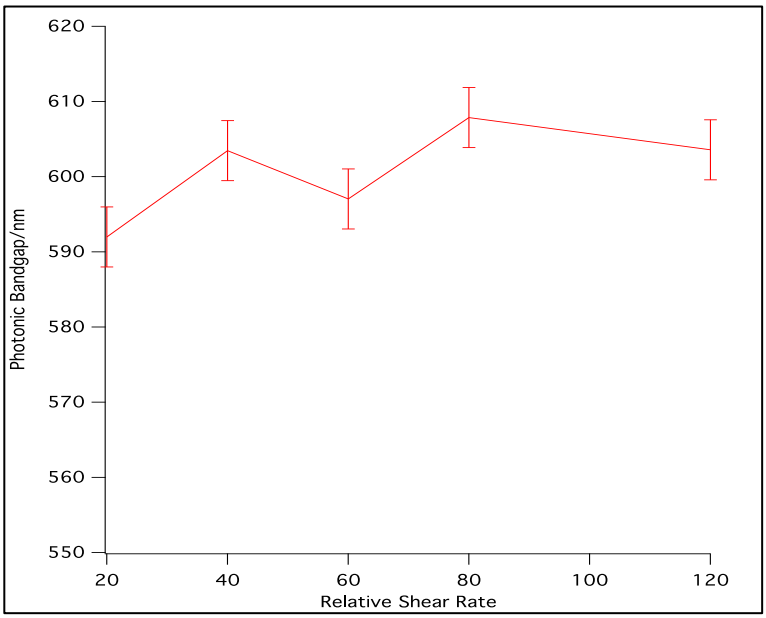

Figure 3-7. Photonic Bandgap with changing the relative shear rate.

3.2.3 Silica Sphere Volume Fraction

The silica spheres volume fraction can also play an important role, which can affect the photonic bandgap. According to the Bragg's Law, which is\

$$2d \times sin\theta = n\lambda, \tag{3-2}$$

where d stands for the distance between to nearby layers, and λ represents the photonic band gap. It cannot be denied that higher concentration of silica sphere leads to a closer distance between to nearby layers. In this case, it can be assumed that the concentration of the silica sphere (the volume fraction of silica spheres) can have an influence on the photonic bandgap.

Prepared the different kinds of colloidal suspension with different volume fraction, which change from 30% to 65%. The plot is shown below in Figure 3-8.

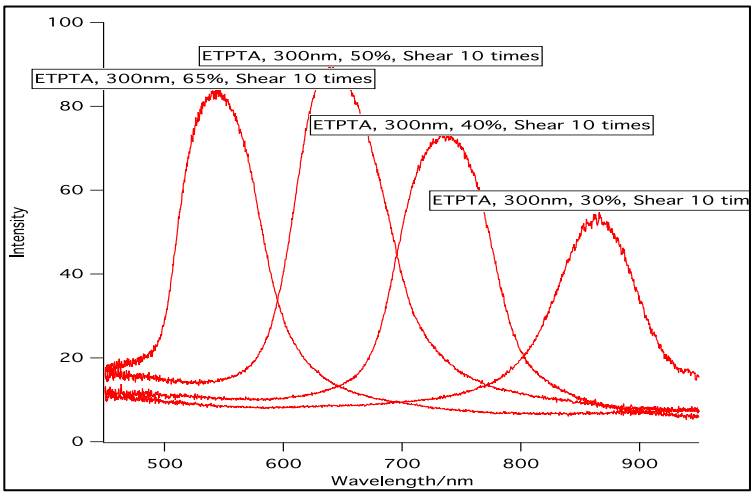

Figure 3-8. Reflection Intensity vs wavelength which varied by silica sphere volume fraction.

3.3 SEM Characterization

During the shear procedure, we can find that the velocity on the top of colloidal suspension had the greatest value of velocity, while the velocity at the bottom is zero. In this case, hypothesis can be obtained that the velocity can make a role to promote the self-assembly. The accuracy of the hypothesis can be testified by SEM characterization.

3.3.1 Cross-sectional SEM

The cross-sectional SEM can tell the influence by the flow rate. SEM images with different depths are listed in Figure 3-9.

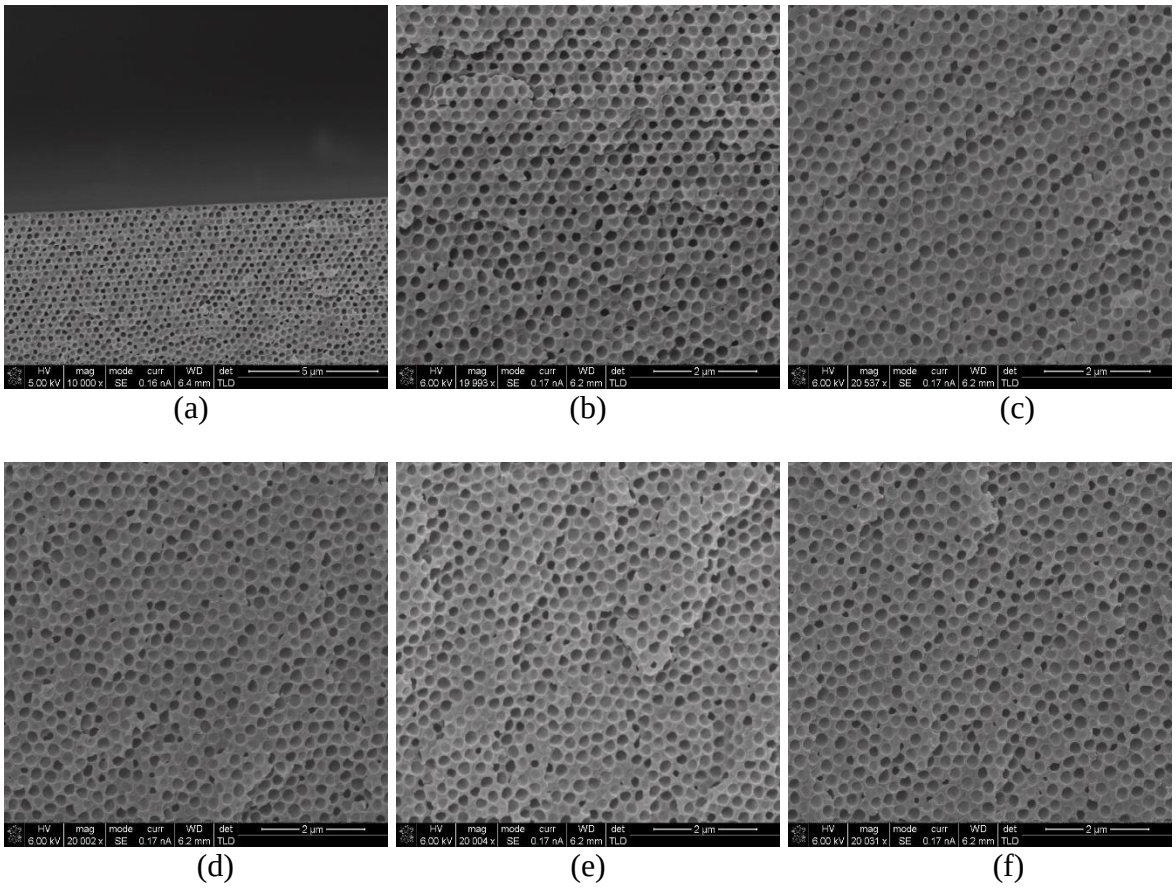

Figure 3-9. ETPTA, 300nm nanoparticle, 50%, shear cycles: 10, relative shear rate: 80: (a)SEM Capture on the top side of ETPTA porous nanocomposite; (b) SEM Capture at the depth of 5μm); (c) SEM Capture at the depth of 12.5μm; (d) SEM Capture at the depth of 25μm; (e) SEM Capture at the depth of 37.5μm; (f) SEM Capture at the depth of 50μm.

The sample in Figure 3-9 is ETPTA nanoprous polymer. It can be seen that top region of the sample shows greater hexagonal order, while the ordering decrease with increasing the depth. This can be explained that the velocity can affect the ordering of the nanospheres.

The fluid on the top shares the same time scale with that on deeper area. In this case, the distance the fluid at the top moves is longer than that at other areas. The shear force will also decay with increasing the depth. In this case, more work is applied at the top of the colloidal suspension, which can be assumed to contribute to the ordering.

3.3.2 Top-plane SEM Characterization

It has already been found that ETPTA nanoporous polymer can achieve great order at the top. Another hypothesis can also be drawn that whether the concentration of silica nanospheres will also contribute to the ordering. Three samples were made with different volume fraction can prove the accuracy of the hypothesis, which is 40%, 50% and 60%. Top layer of the sample can be etched off by plasma etching. Let gold embedded the samples to increase the electroconductivity. The SEM images of different samples are listed in Figure 3-10.

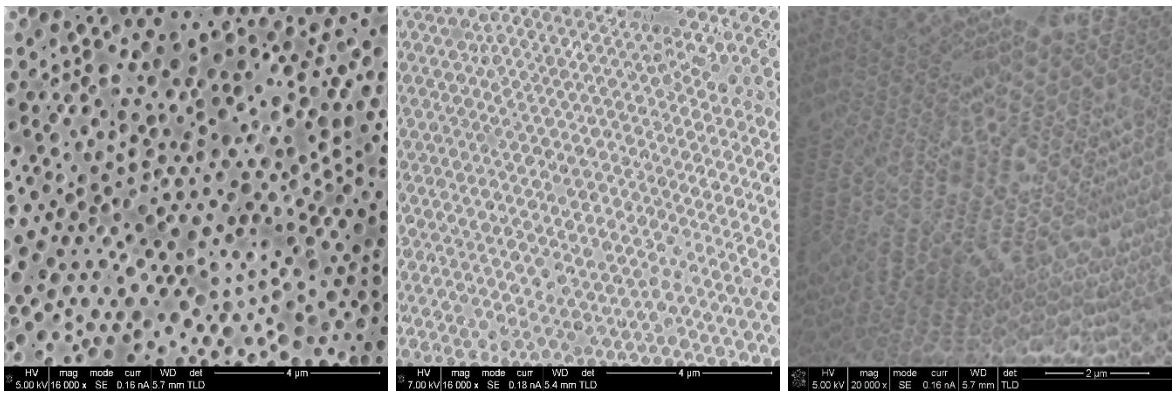

(a) (b) (c)

Figure 3-10. SEM images of ETPTA nanoporous polymer (300nm) on the top plane: (a) volume fraction: 40%; (b) volume fraction: 50%; (c) volume fraction: 65%.

From Figure 3-10, result can be found that higher concentration will promote the ordering of the porous structure. Besides, it can also easily to be seen that higher the concentration of nanoparticles is, closer the distance between two nearby particles is, which can greatly match the Bragg's Law,

$$2n_{eff}dsin\theta = \lambda_{peak}, \tag{3-3}$$

which higher concentration of nanoparticle will lead to a blue shift.

CHAPTER 4
MODELING OF TRANSPORT ANALYSIS

In order to simplify the problem, the whole experiment can be divided into two procedures, which is squeeze procedure and shear procedure. In the squeeze procedure, two glass substrates moved towards, which led to a squeeze flow. The velocity of the flow, the pressure and force exerted on the glass substrate could be solved. In the shear procedure, the glass substrate beneath is immobile while the upper glass substrate shears the colloidal suspension with shear force, which helps to achieve mass transport. The detail analysis will be further demonstrated below.

4.1 Squeeze Procedure

In the squeeze procedure, the two glass substrates were brought together with the help of pressure, which led to the squeeze flow in colloidal suspension radially between two glass substrates. The squeeze flow cannot be unidirectional flow because of the continuity equation of continuous flow. One was r-direction while the other was z-direction.

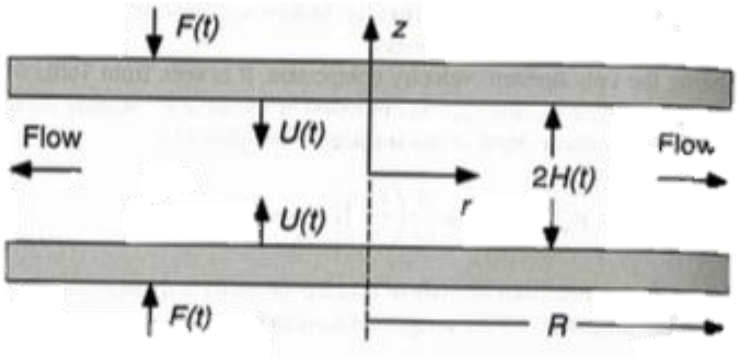

Figure 4-1. Schematic graph for squeeze geometry.

The force exerted on each glass substrate led to the velocity of the glass substrate U(t). Assumed that the substrates separation is 2H(t). In this case, $U(t) = -dH(t)/dt$. Besides, it should be assumed that the edge effect was negligible to obtain the creeping flow between two glass substrates, which meant that $Re = H_0 U_o \rho/\mu \ll 1$, and $H_0/R \ll 1$, where H_0 was initial

distance between the upper substrate and midline and R represented radius characteristic length scale. Moreover, assumed that the geometry was symmetric, which meant that the velocity in θ direction equaled to 0 ($v_\theta = 0$). Also, it could be assumed that the dynamic pressure $\mathcal{P} = 0$ at the edge of the fluid, where the fluid existed.

The time scale imposed by the movement of glass substrate $t_p = H_0/U_0$ shared the same order of magnitude with the convection times scale, which meant that $Sr = t_p/t_c = 1$. In this case, that $Re \ll 1$ was needed to let $Re/Sr \ll 1$ to justify a pseudosteady state. From the analysis above, $H_0/R \ll 1$ was necessary to neglect the edge effect, which meant that the fluid was almost unidirectional. As a consequence, the ratio of velocity in z-direction and velocity in r-direction was much smaller than 1 ($v_z/v_r \ll 1$), because v_z/v_r shared the same order of magnitude with H_0/R. In this case, r-component of Navier-Stokes Equation was necessary to be focused on. The small gap led to the validation of lubrication approximation. According to r-component of Navier-Stokes Equation,

$$0 = -\frac{\partial \mathcal{P}}{\partial r} + \mu \frac{\partial^2 v_r}{\partial z^2} \tag{4-1}$$

where μ is the viscosity of the fluid, which was tested as a constant according to the rheology measurement. The boundary conditions were listed below

$$\frac{\partial v_r}{\partial z} = 0 \; at \; z = 0; \; v_r = 0 \; at \; z = H. \tag{4-2}$$

Integrating the Navier-Stokes Equation and applying boundary conditions gives,

$$v_r = -\frac{H^2}{2\mu}\frac{\partial \mathcal{P}}{\partial r}\left[1 - \left(\frac{z}{H}\right)^2\right]. \tag{4-3}$$

Found that the radial velocity depended upon r by $\frac{\partial \mathcal{P}}{\partial r}$ and depended on t by H and $\frac{\partial \mathcal{P}}{\partial r}$. $\frac{\partial \mathcal{P}}{\partial r}$ term could be eliminated by integrating continuity equation $\frac{1}{r}\frac{\partial}{\partial r}(rv_r) + \frac{\partial v_z}{\partial z} = 0$ over z,

$$v_z(r,z,t) = \int_0^z \frac{1}{r}\frac{\partial}{\partial r}(rv_r)\,dZ,. \tag{4-4}$$

where Z represented dummy variable. The boundary conditions for v_z could be obtain by the fact, which were given as

$$v_z = 0\ at\ z = 0; v_z = -U\ at\ z = H. \tag{4-5}$$

The pressure gradient could be solved as

$$\frac{\partial \mathcal{P}}{\partial r} = -\frac{3}{2}\frac{\mu U r}{H^3}. \tag{4-6}$$

The dynamic pressure could be solved under the boundary condition that $\mathcal{P} = 0$ at r = R, which was written as

$$\mathcal{P}(r,t) = \frac{3}{4}\frac{\mu U r}{H^3}\left[1 - \left(\frac{r}{R}\right)^2\right]. \tag{4-7}$$

Then the applied force could be solved with the help of dynamic pressure, which was given as

$$F(t) = 2\pi\int_0^R \mathcal{P}(r,t)\,rdr = \frac{3\pi}{8}\frac{\mu U R^4}{H^3}. \tag{4-8}$$

From the expression of applied force, found that *U* must decrease if F was held constant or F must increase if U is held constant, because H decreased with time. The final expression for velocity component are

$$v_r(r,z,t) = \frac{3}{4}U\left(\frac{r}{H}\right)\left[1 - \left(\frac{z}{H}\right)^2\right], \tag{4-9}$$

$$v_z(r,z,t) = -\frac{3}{2}U\left[\left(\frac{z}{H}\right) - \frac{1}{3}\left(\frac{z}{H}\right)^3\right]. \tag{4-10}$$

4.2 Shear Procedure

Shear procedure existed after the squeeze procedure, and shear force was applied to colloidal suspension by moving the upper glass substrate. The upper glass substrate moved with the help of KD Scientific Syringe Pump, which could control same shear rate during shearing procedure. Since the upper glass substrate moved back and forth, rectangular coordinate was

applied to the system. It should be assumed that the fluid was unidirectional. In this case, *x*-component of Navier-Stokes Equation should be focus on, which was written as

$$\frac{d^2 v_x}{dy^2} = \mu \frac{d\mathcal{P}}{dx}. \tag{4-11}$$

Set the original point at the bottom plane, the boundary conditions for v_x were written below

$$v_x = U \; at \; y = 2H; \; v_x = 0 \; at \; y = 0. \tag{4-12}$$

Integrating the Navier-Stokes Equation gave the velocity expression, which was written as

$$v_x = \frac{H^2}{2\mu} \frac{d\mathcal{P}}{dx} \left[\left(\frac{y}{H} \right)^2 - 2 \left(\frac{y}{H} \right) \right] + \frac{U}{2} \left(\frac{y}{H} \right). \tag{4-13}$$

Introduced mean velocity of the colloidal suspension between two glass substrates V, which could be tested by introducing probe beads in the colloidal suspension. In this case, term "$d\mathcal{P}/dx$" could be eliminated by mean velocity V.

Integrate velocity v_x over *y* from 0 to 2H, got

$$2VH = \int_0^{2H} v_x \, dy. \tag{4-14}$$

Substituted v_x with the solution above,

$$\frac{d\mathcal{P}}{dx} = \frac{3\mu(2V - U)}{H^2}. \tag{4-15}$$

$$v_x = \frac{3(2V - U)}{8} \left[\left(\frac{y}{H} \right)^2 - 2 \left(\frac{y}{H} \right) \right] + \frac{U}{2} \left(\frac{y}{H} \right). \tag{4-16}$$

CHAPTER 5
RESULT AND DISCUSSION

Silica spheres are fabricated with Stöber Method, which have a diameter variation of 5%. Silica spheres are placed in ETPTA monomer with certain volume fraction, which varies from 30% to 65%. The monomer will polymerize with the help of photoinitiator Darocur 1173. As a result, 2 vol% photoinitiator Darocur 1173 is also needed. The colloidal suspension can be transparent because the Refractive Index of silica sphere (RI = 1.42) is similar with that of ETPTA (RI = 1.46). The silica spheres are negatively charged, which is the main reason for silica spheres to achieve self-assembly. The interaction (electrostatic repulsion) among silica spheres can also stabilize the colloidal suspension for few weeks.

Two glass substrates move relatively to shear the colloidal suspension. Spacer will help to control the thickness. The shear rate can be controlled by KD Scientific Syringe Pump. The uniform glass substrate can offer a uniform shear rate and geometry. The monomer/crystal colloidal suspension can be polymerized when exposed under the UV radiation to become polymer/crystal nanocomposite. Submerged in 2% HF solution, silica nanospheres can be etched and porous polymer forms.

The experiment can be divided into two procedures, which is squeeze procedure and shear procedure, respectively. Those two procedures can make the problem much easier to manipulate. During the squeeze procedure, two glass substrates move toward to squeeze the colloidal suspension. The fluid cannot be unidirectional because of the continuity properties of continuous fluid. As a result, the directions of the flow are not only on axial direction, but also on radial direction. The velocity in both axial and radial direction can be solved by Navier-Stokes Equation in Cylindrical Coordinate. The dynamic pressure can be solved by integration of

continuity equation. Therefore, the applied force can be calculated by integration of the dynamic press over area,

$$F(t) = 2\pi \int_0^R \mathcal{P}(r,t)\, r dr = \frac{3\pi}{8} \frac{\mu U R^4}{H^3}. \quad (5\text{-}1)$$

From the expression of applied force, found that *U* must decrease if F was held constant or F must increase if U is held constant, because H decreased with time. From the expression of applied force, find that applied force is a function of the substrate velocity while the velocity of the glass substrate is a function of time. As a consequence, the applied force is a function of time.

The shear procedure can be analyzed in Rectangular Coordinate because the flow is unidirectional because the movement of glass substrate is unidirectional. Shear procedure can be applied to align the silica sphere with the diameter from 100nm to 1000nm, which can be easily fabricated by Stöber method. Considering different colloidal suspensions with same volume fraction with different diameter, find that greater the diameter of the silica sphere is, less dilute the colloidal suspension is.

We attribute to the optical properties of the porous polymer. Shining reflection can be found on the sample. In this case, we concentrated on the value of phontic bandgap. During the spectrum characterization, it is really important to control other variables with changing the main variable, such as thickness and diameter of the silica sphere, which is about to be tested. As for spectrum result, it can hardly be seen that the shear rate and shearing cycle can make much contribution to the spectrum properties, which means that it is not the main factor that can contribute the spectrum properties, such as the photonic bandgap, bandwidth, etc. What really matters is the concentration of silica sphere. Phenomenon can be easily seen from the spectrum result that higher the volume fraction of silica sphere is, more significant the blue-shift is, which

means that the value of photonic bandgap will decrease with increasing the volume fraction of silica spheres. This phenomenon can be well explained by the Bragg's Law, which is given as $2n_{eff}dsin\theta = \lambda_{peak}$, where $sin\theta = 1$ at normal incidence, and *d* stands for the interlayers spacing gap. λ_{peak} represents the value of photonic bandgap and n_{eff} belongs to effective refractive index of the mediate, which is written as$n_{eff} = n_1 f_1 + n_2 f_{2,}$where n_1 and n_2 are the refractive indices of the different materials, and f_1 and f_2 represent the volume fraction of the component.

Under the condition that the diameter of silica nanospheres stay the same, higher volume fraction of silica sphere leads to smaller gap between two nearby layers, which can decrease the reflection wavelength λ_{peak}. However, the value of photonic bandgap cannot be linearly decrease with linearly increase the volume fraction of silica sphere. The reflection wavelength cannot be always decrease with increasing the concentration of silica nanospheres, and it will stay constant after the concentration of silica nanosphere reaches a certain value. In this case, the silica nanosphere is saturated throughout colloidal suspension. When the concentration is really high, the colloidal suspension can be polymerized to a gel, which is really hard to be manipulated.

The main reason why shear rate cannot be the main factor to determine the Photonic bandgap can be explained by rheology measurement. According to the rheology measurement, the viscosity of colloidal suspension stays constant when shear rate reaches a certain value, which is approximately 20 s^{-1} from the rheology plot. The speed ranging from ~ $0.1\mu m/s$ to $1mm/s$, which is much larger than $20s^{-1}$ (shear rate). In this case, the viscosity can be assumed as a constant value, which means that the colloidal suspension is a Newtonian Fluid. This can

explain the reason why the shear rate cannot affect the photonic bandgap of the ETPTA porous sample.

From the modeling in shear procedure, suspension on the top side has the greater velocity, while the bottom suspension has the lower velocity. From SEM characterization (Figure 3-7), find that the pores on the top side have regular nanostructure. Different SEM captures at different areas can tell the regular phenomenon. It can be found that the quality of nanostructure can be improved by enhancing the flow velocity, which means that higher velocity of the fluid, highly ordered the nanostructure is. SEM captures can be shown in Figure 3-7 and Figure 3-8.

CHAPTER 6
CONCLUSION

Shear coating technology could not only be applied for glass substrate, but also be utilized in industrial field. What's more, shear coating shows its potential in different areas, such as manipulating structural colors, materials in chromatography, etc. The main point of the experiment belongs to the fabrication of colloidal suspension, which has various application, such as the fabrication of opals. We also find that the colloidal suspension can also be applied in a mold technology. However, dry stress is the main point for our future research. Moreover, whether Shape Memory Effect material can be applied to the Shear Coating technology is also important.

LIST OF REFERENCES

1. Mayoral, R.; Requena, J.; Moya, J. S.; Lopez, C.; Cintas, A.; Miguez, H.; Meseguer, F.; Vazquez, L.; Holgado, M.; Blanco, A. Adv. Mater. 1997, 9, 257.

2. Vlasov, Y. A.; Bo, X. Z.; Sturm, J. C.; Norris, D. J. Nature 2001, 414, 289.

3. Denkov, N. D.; Velev, O. D.; Kralchevsky, P. A.; Ivanov, I. B.; Yoshimura, H.; Nagayama, K. Nature 1993, 361, 26.

4. Jiang, P.; Bertone, J. F.; Hwang, K. S.; Colvin, V. L. Chem. Mater. 1999, 11, 2132.

5. Wong, S.; Kitaev, V.; Ozin, G. A. J. Am. Chem. Soc. 2003, 125, 15589.

6. Holtz, J. H.; Asher, S. A. Nature 1997, 389, 829.

7. Van Blaaderen, A.; Ruel, R.; Wiltzius, P. Nature 1997, 385, 321.

8. Park, S. H.; Xia, Y. N. Langmuir 1999, 15, 266.

9. Ge, J. P.; Yin, Y. D. J. Mater. Chem. 2008, 18, 5041.

10. Hayward, R. C.; Saville, D. A.; Aksay, I. A. Nature 2000, 404, 56.

11. Wu, Y. L.; Derks, D.; van Blaaderen, A.; Imhof, A. Proc. Natl. Acad. Sci. U.S.A. 2009, 106, 10564.

12. Shereda, L. T.; Larson, R. G.; Solomon, M. J. Phys. Rev. Lett. 2008, 101, 038301.

13. Jiang, P.; McFarland, M. J. J. Am. Chem. Soc. 2004, 126, 13778.

14. Mahoney L; Koodali RT. 2014 Mar 31;7(4):2697-2746. doi: 10.3390/ma7042697.

15. H, Yang; P. Jiang. Langmuir 2010, 26(16), 13173–13182.

16. Mistler, R. E.; Twiname, E. R. Tape Casting: Theory and Practice; American Ceramic Society: Westerville, OH, 2000.

17. Chou, Y. T.; Ko, Y. T.; Yan, M. F. J. Am. Ceram. Soc. 1987, 70, C280.

18. Loest, H.; Lipp, R.; Mitsoulis, E. J. Am. Ceram. Soc. 1994, 77, 254.

19. Pitchumani, R.; Karbhari, V. M. J. Am. Ceram. Soc. 1995, 78, 2497.

20. Kim, H. J.; Krane, M. J. M.; Trumble, K. P.; Bowman, K. J. J. Am. Ceram. Soc. 2006, 89, 2769.

BIOGRAPHICAL SKETCH

Zhen Liu completed his undergraduate education from Dalian University of Technology and obtained his bachelor degree in Chemical Engineering in May 2016. He also completed his project at University of California, Berkeley as a transfer student in 2014. While working in Dr. Peng Jiang's lab, Zhen Liu obtained his master's degree from University of Florida in the fall of 2017.